Food and Chemical Toxicology 134 (2019) 110791

Contents lists available at ScienceDirect

Food and Chemical Toxicology

journal homepage: www.elsevier.com/locate/foodchemtox

Deltamethrin promotes adipogenesis via AMPKα and ER stress-mediated pathway in 3T3- L1 adipocytes and *Caenorhabditis elegans*

Li Yuan[a,1], Jie Lin[a,1], Yuejia Xu[b], Ye Peng[a,b], John M. Clark[c], Ruichang Gao[a], Yeonhwa Park[b,*], Quancai Sun[a,**]

[a] School of Food and Biological Engineering, Jiangsu University, Zhenjiang, Jiangsu Province, 212013, China
[b] Department of Food Science, University of Massachusetts, Amherst, MA, 01003, United States
[c] Department of Veterinary and Animal Sciences, University of Massachusetts, Amherst, MA, 01003, United States

ARTICLE INFO

Keywords:
Deltamethrin
Pyrethroid
Adipogenesis
AMPKα
ER stress

ABSTRACT

Previous research has shown that deltamethrin, a Type-II pyrethroid, increases fat accumulation in adipocytes and *Caenorhabditis elegans*. The underlying mechanisms on how deltamethrin promotes fat accumulation, however, are unknown. The aim of the current study was therefore to determine the possible mechanisms through which deltamethrin increases fat accumulation in mouse 3T3-L1 adipocytes and *C. elegans*. Deltamethrin (10 μM) significantly increased fat accumulation, and the expression of adipogenic regulators, such as CCAAT/enhancer-binding protein (C/EBPα) and fatty acid synthase (FAS). Deltamethrin significantly decreased the phosphorylation of AMP-activated kinase α (AMPKα), while it increased protein expression of endoplasmic reticulum (ER) stress markers in 3T3-L1 adipocytes and *C. elegans*. The activation of AMPK with 5-aminoimidazole-4-carboxamide ribonucleotide (AICAR) or the inhibition of ER stress with 4-phenylbutyrate (4-PBA) abolished the effects of deltamethrin on adipogenesis. Further study reveals that 4-PBA recovered the decreased AMPK phosphorylation induced by deltamethrin. These results suggest that deltamethrin promotes adipogenesis through an ER stress-AMPKα mediated pathway.

1. Introduction

Pyrethroid insecticides are synthetic derivatives of naturally occurring pyrethrins, which are widely used in agriculture and households for the control of pests. Due to their relatively low mammalian toxicity (Armstrong et al., 2013; Yoon et al., 2008), pyrethroid insecticides, a relatively new class, are regarded as safe compared to carbamates/organophosphates. Pyrethroids have been intensively used in Europe and the United States since the early 1980s (Kim et al., 2010), and significant amounts of pyrethroid metabolites have been detected in the urine of humans, including pregnant women and children in recent years (Berkowitz et al., 2003; Morgan et al., 2007; Naeher et al., 2010). By the mid-1990s, pyrethroids occupied about 23% of the global insecticide market; this decreased to around 15% in 2015 (Xiao et al., 2017b).

Pyrethroids are divided into two classes according to their structure and toxic effects (Gammon et al., 1981). Type I compounds have no cyano group on the methylene carbon of the phenoxybenzyl alcohol, and they can cause tremors or skin parathesia. Type II compounds contain a cyano group, and their toxic symptoms include salivation and hyperexcitability (Kim et al., 2008). As excitoxins, pyrethroids achieve their toxicity by preventing the closure of voltage-sensitive sodium channels (VSSC) in nerve cells (Choi and Soderlund, 2006). Deltamethrin is a type II pyrethroid, and their LD_{50} varies from 30 mg/kg body weight (in an oily vehicle) to 5000 mg/kg body weight (in an aqueous vehicle) (Shen et al., 2017). The elimination half-life of deltamethrin was 38.5 h in rats when administered orally, and 33.0 h if administered intravenously (Anadon et al., 1996). Deltamethrin was reported to accumulate in various tissues, including plasma, brain, fat, skin and muscle (Berkowitz et al., 2003; Morgan et al., 2007; Naeher et al., 2010).

Emerging evidence, including our previous studies, suggests a relationship between exposure to insecticides that cause membrane depolarization and the development of obesity (Kim et al., 2014, 2016; Mangum et al., 2015; Park et al., 2013; Sun et al., 2016a, 2017, 2018a; Xiao et al., 2017a, 2018). Deltamethrin was previously reported to

* Corresponding author. University of Massachusetts, 102 Holdsworth Way, Amherst, MA, 01003, United States.
** Corresponding author. Jiangsu University, Zhenjiang, Jiangsu Province, 212013, China.
E-mail addresses: ypark@foodsci.umass.edu (Y. Park), sqctp8@ujs.edu.cn (Q. Sun).
[1] These authors contributed equally to the present work.

https://doi.org/10.1016/j.fct.2019.110791
Received 13 June 2019; Received in revised form 21 August 2019; Accepted 23 August 2019
Available online 30 August 2019
0278-6915/

enhance adipogenesis and decrease the phosphorylation of AMP-activated protein kinase-α (AMPKα) in mouse 3T3-L1 adipocytes and *C. elegans* (Shen et al., 2017), although the underlying mechanisms remained to be determined.

AMPK is a master regulator of energy metabolism and lipid synthesis. Activation of AMPK has been reported to inhibit adipogenesis with reduced expression of CAATT element binding protein-α (C/EBPα) and Fatty acid synthase (FAS) (Habinowski and Witters, 2001). ER stress also known as the unfolded protein response (UPR) has also been linked with obesity and UPR activation contributes to adipogenesis (Basseri et al., 2009). The aim of the current study was therefore to determine the role of ER stress in deltamethrin-induced AMPK inactivation, leading to enhanced adipogenesis in 3T3-L1 adipocytes and the *C. elegans* model.

2. Materials and methods

2.1. Materials

Mouse 3T3-L1 preadipocytes were provided by the Shanghai Cell Bank of the Chinese Academy of Sciences (Shanghai, China). Fetal bovine serum (FBS), Dulbecco's modified Eagle's medium (DMEM), insulin, methylisobutylxanthin, dexamethasone, dimethyl sulfoxide (DMSO), 5-aminoimidazole-4-carboxamide ribonucleotide (AICAR, ≥98%), and sodium phenylbutyrate (4-PBA, ≥98%) were obtained from Sigma-Aldrich Co. (St. Louis, MO, USA). Deltamethrin [Cyano(3-phenoxyphenyl)methyl 3-(2,2-dibromovinyl)-2,2-dimethylcyclopropanecarboxylate] (≥99%) was purchased from AccuStandard (New Haven, Connecticut, USA). Radioimmuno-precipitation assay (RIPA) buffer supplemented with 1% protease and phosphatase inhibitor was purchased from Beyotime Biotechnology Inc. (Shanghai, China). Rabbit antibodies to AMPKα, phosphorylated AMPKα (pAMPKα), FAS, C/EBPα, adiponectin, binding immunoglobulin protein (Bip), CCAAT-enhancer-binding protein homologous protein (CHOP), activating transcription factor 6 (ATF6), inositol-requiring enzyme 1 α (IRE1α), X-box binding protein 1s (XBP1s), glyceraldehyde 3-phosphate dehydrogenase (GAPDH), and horseradish peroxidase-conjugated goat anti-rabbit IgG were from Cell Signaling Technology (Beverly, MA, USA). Rabbit antibodies of phosphorylated IRE1α were obtained from Abcam (Cambridge, MA, USA). All the *C. elegans* strains and *Escherichia coli* OP50 used in the current study were obtained from *Caenorhabditis* Genetics Center (CGC), University of Minnesota, City, USA. Strains used include SJ4005 [*zcIs4* (*phsp-4*::*GFP*)]; AM141[*rmIs133* (*unc-54p*::*Q40*::*YFP*)]. Household Clorox bleach (The Clorox Company, Oakland, CA, USA) was used for synchronizing the worms. Fluorodeoxyuridine (FUdR) and carbenicilin were purchased from Sigma-Aldrich Co. (St. Louis, MO, USA).

2.2. 3T3-L1 culture

3T3-L1 preadipocytes were cultured as previously described (Park et al., 2013; Peng et al., 2019c). 3T3-L1 preadipocytes were maintained in DMEM supplemented with 10% FBS at 37 °C until confluence. Adipocyte differentiation was initiated with DMEM containing 10% FBS and a mixture of dexamethasone (1 μM), methylisobutylxanthin (0.5 mM), and insulin (1 μg/mL). On day 2, the medium was switched to DMEM with 10% FBS and insulin. From day 4, cells were maintained in DMEM plus 10% FBS, and the medium was changed at 2-day intervals. Cells were treated with deltamethrin (1 and 10 μM), AICAR (40 μM) or 4-PBA (10 mM) from day 0 as indicated in each figure legend. The deltamethrin, AICAR and 4-PBA concentrations used in the current study were based on previous publications (Basseri et al., 2009; Shen et al., 2017; Sun et al., 2016a, 2017) and had no cytotoxicity on 3T3-L1 adipocytes as determined by MTT assay (Fig. 1S).

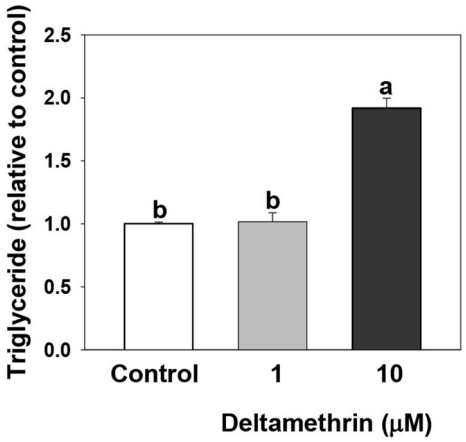

Fig. 1. Deltamethrin treatment increased triglyceride accumulation in 3T3-L1 adipocytes. Cells were treated with deltamethrin for 8 days (from day 0). Numbers are mean ± S.E. (n = 4). Means with different letters were significantly different at $P < 0.05$.

2.3. Measurement of cell cytotoxicity

MTT-based cell viability test was performed to determine the cytotoxicity of deltamethrin, AICAR, and 4-PBA. Briefly, 3T3-L1 cells were seeded in 96-well plates at a density of 1×10^6 cells/mL. Cells were treated with deltamethrin, AICAR (40 μM) or 4-PBA (10 mM) for 8 days. The medium was then replaced with 5 mg/mL MTT in DMEM (without phenol red) for 4 h at 37 °C. After incubation, and 3 times wash with phosphate-buffered saline (PBS), formazan crystals dissolved in DMSO were measured with Multiskan FC microplate reader (Thermo Fisher Scientific, Waltham, MA, USA) at 570 nm.

2.4. Triglyceride quantification

Cells were washed three times with phosphate-buffered saline (PBS) and harvested by scraping in PBS supplemented with 1% Triton-X after 8 days of differentiation. Homogenous samples were obtained from cells after sonication. The triglyceride (TG) and protein contents were quantified with kits from Nanjing Jiancheng Bioengineering Institute (Nanjing, Jiangsu Province, China). TG content was normalized with protein concentration.

2.5. Immunoblotting

Cells were lysed with RIPA buffer supplemented with protease and phosphatase inhibitor and immunoblotting was performed as previously described (Peng et al., 2019b; Sun et al., 2018b). Primary rabbit antibodies were diluted following the recommendation of producers. Horseradish peroxidase conjugated goat anti-rabbit IgG was used as the secondary antibody. Detections were performed on an image station Tanon 5500 (Shanghai, China) with ECL Substrate Kit from Beyotime Biotechnology Inc. (Shanghai, China). Image and results were analyzed with Image J software (Schneider et al., 2012).

2.6. C. elegans culture

C. elegans were cultured using standard methods as previously described (Peng et al., 2019a; Sun et al., 2016b). Nematode growth medium (NGM), M9-buffer solution, and S-complete solution were prepared as previously reported (Shen et al., 2017; Sun et al., 2016b). Briefly, after a synchronous worm population was acquired, synchronized L1 worms were cultured in 12-well plates at 25 °C treated with 0.1% DMSO as control, or 25 μM deltamethrin, determined based on preliminary experiments that 10 μM deltamethrin only mildly increased

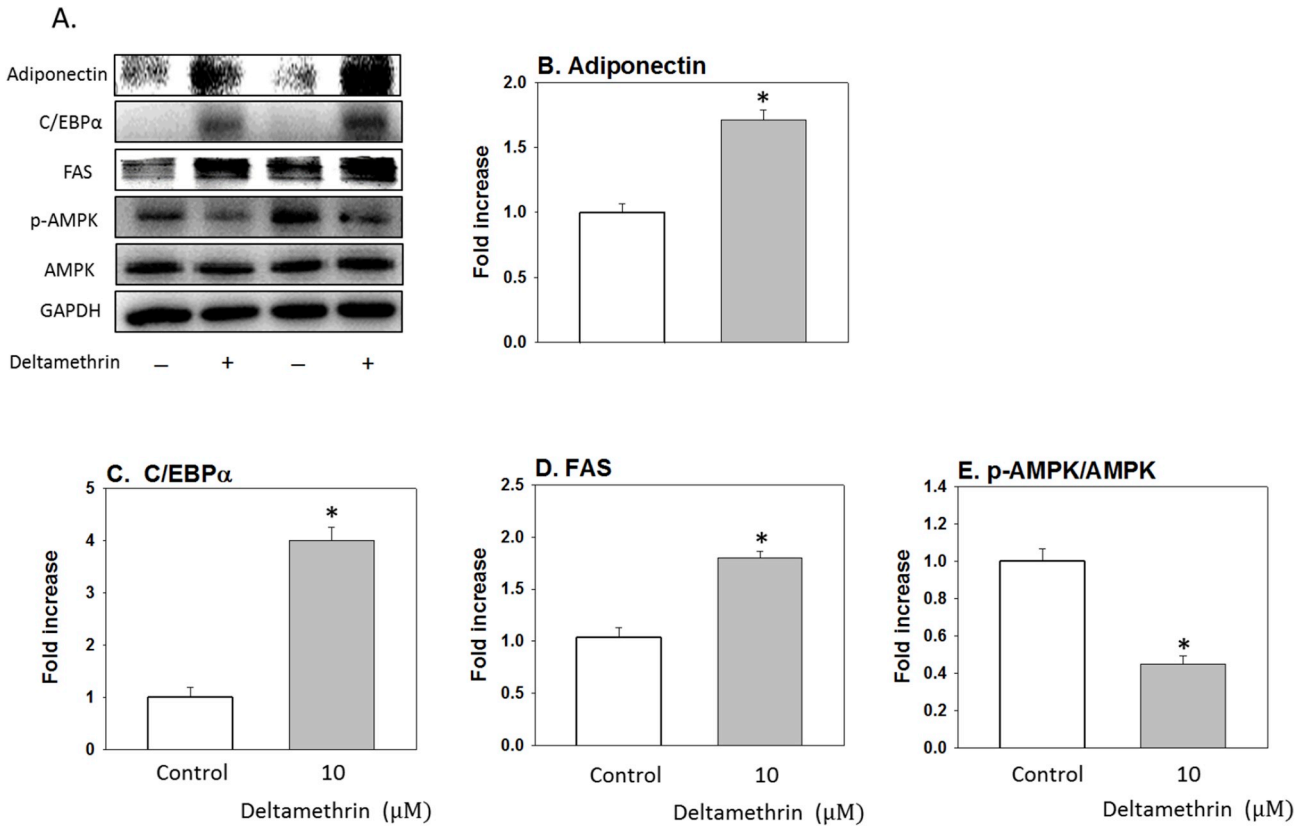

Fig. 2. Effects of deltamethrin on protein levels of adipogenic regulators. A. representative picture; B. Adiponectin; C. C/EBPα, CAATT element binding protein-α; D. FAS, Fatty acid synthase; E. pAMPKα/AMPKα, phosphorylated AMP-activated protein kinase-α over AMPKα. Cells were treated with deltamethrin (10 μM) for 8 days (from day 0). Numbers represent mean ± S.E. (n = 3–4). * $P < 0.05$, *vs.* control.

the hsp-4 expression by 9.6% ($P = 0.06$) (Fig. 2S).

2.7. Fluorescence microscopy

Before imaging, worms were immobilized in 2 mM levamisole, and mounted on a slide with 3% agarose using a cover slip. After preparation of the slides, fluorescent images were taken using a Nikon Eclipse Ti-U Inverted Microscope (Micro Video Instruments, Avon, MA). The average GFP intensity of SJ4005 worms was measured for ER stress response, and the average number and size of polyglutamine yellow fluorescence protein (YFP) inclusions were scored for AM141 worms. For each treatment, about 30 worms were used. Analysis of the images was performed using the ImageJ software developed by the National Institute of Health (NIH).

2.8. Statistical analyses

The PROC MIXED procedure was utilized to analyze data with the SAS software (version 9.3, SAS Institute Inc., Cary, NC, USA). Differences between each treatment in Figs. 1, 3, 5 and S1 were analyzed using one-way ANOVA (Tukey's multiple-range test). Two-way ANOVA along with a LS means statement was used in Figs. 3 and 5. Significance of differences was defined at the $P < 0.05$ level.

3. Results

3.1. Deltamethrin increased triglyceride content and protein expression of regulators controlling adipogenesis in 3T3-L1 adipocytes

Consistent with the previous report (Shen et al., 2017), deltamethrin (10 μM) treatment significantly increased TG content by 91% ($P = 0.0001$) compared to the control in this cell-based model (Fig. 1). Deltamethrin also significantly increased the protein expression levels of adiponectin, C/EBPα and FAS (Fig. 2A & D), meanwhile reduced the phosphorylation of AMPKα compared to the control (Fig. 2A & E). These results suggest that deltamethrin induced adipogenesis and reduced the activation of AMPKα in 3T3-L1 adipocytes.

3.2. Influence of AMPKα activation on adipogenesis induced by deltamethrin

We further investigated the influence of AMPKα activation on increased adipogenesis induced by deltamethrin. AICAR is a potent AMPK activator that is phosphorylated to generate 5-amino-4-imidazole-carboxamide ribotide (ZMP). ZMP mimics AMP and stimulates AMPK phosphorylation in the cell (Merrill et al., 1997). As shown in Fig. 3A–B, there was a significant interaction between AICAR and deltamethrin treatment ($P = 0.0094$) on AMPK phosphorylation. AICAR increased AMPK phosphorylation both in the absence (71%, $P = 0.0014$) or the presence of deltamethrin (300%, $P < 0.0001$), suggesting that AICAR successfully activated AMPK in the current system. There was a significant interaction between AICAR and deltamethrin treatment on fat accumulation ($P = 0.0002$). AICAR treatment alone decreased fat accumulation (53%, $P = 0.0036$), while 10 μM deltamethrin treatment alone increased fat accumulation (100%, $P < 0.0001$), as shown in Fig. 3C. When cells were treated with AICAR and deltamethrin together, the enhanced fat accumulation by deltamethrin was abolished by AICAR treatment ($P < 0.0001$) (Fig. 3C). These results suggest that deltamethrin induced fat accumulation via the AMPKα-dependent pathway.

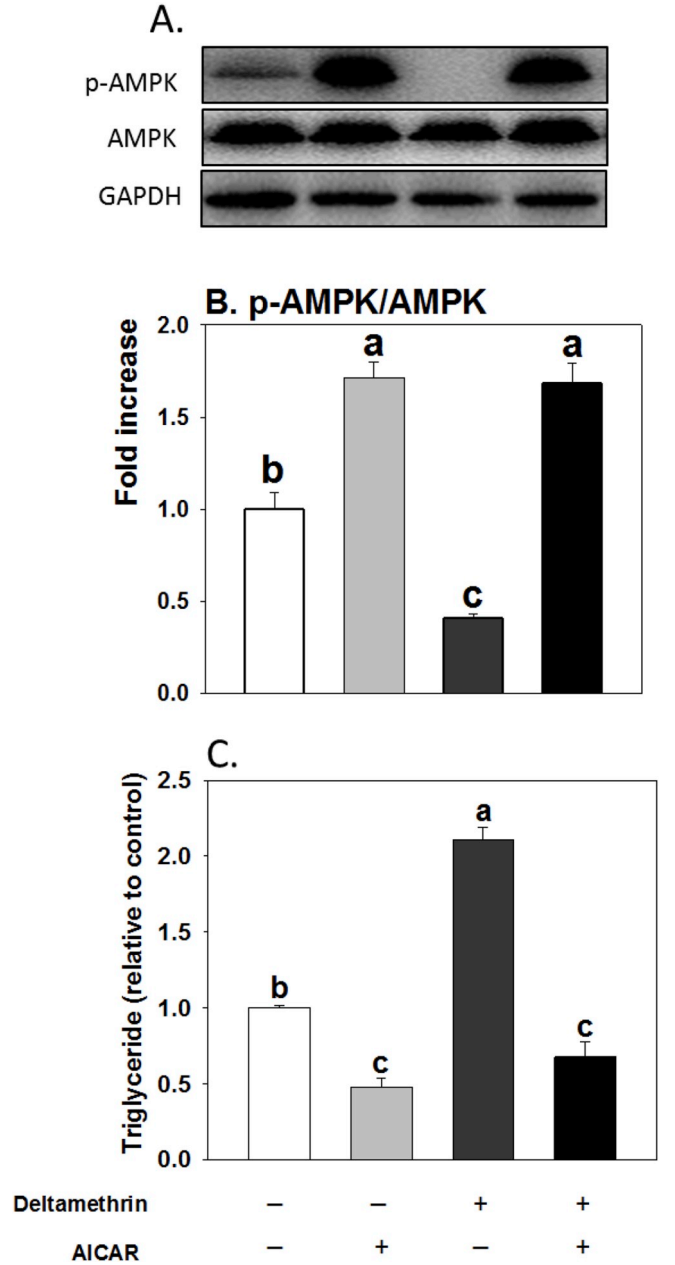

Fig. 3. AICAR (5-Aminoimidazole-4-carboxamide ribonucleotide) abolished the increased fat accumulation induced by deltamethrin. A. representative picture; B. pAMPKα/AMPKα, phosphorylated AMP-activated protein kinase-α over AMPKα; C. Triglyceride content. Cells were treated with deltamethrin (10 μM) or AICAR (40 μM) for 8 days (from day 0). Numbers represent mean ± S.E. (n = 3). Means with different letters were significantly different at $P < 0.05$.

3.3. Deltamethrin treatment stimulated ER stress in 3T3-L1 adipocytes

BiP, a molecular chaperone in the lumen of ER, binds to newly synthesized or misfolded proteins and helps in the subsequent folding, oligomerization, or degradation of these proteins (Cnop et al., 2012). ATF6 is an ER-stress-regulated transmembrane transcription factor that activates the transcription of ER molecular chaperones. Upon ER stress, BiP dissociates with ATF6, and allows the translocation of ATF6 to the Golgi, which then localizes into the nucleus to activate UPR target genes, including adipogenic genes (Ho et al., 2018; Shen et al., 2002). Reduction of ATF6 expression resulted in impaired expression of key adipogenic genes and reduced fat accumulation (Lowe et al., 2012). Deltamethrin (10 μM) treatment significantly increased the protein expression of BiP and ATF6 compared to the control (140% & 100%, $P = 0.0100$ & 0.0038, respectively, Fig. 4A-C). IRE1α is another ER-resident transmembrane protein containing a luminal domain and a cytoplasmic portion with a protein kinase domain. Upon ER stress, IRE1α undergoes trans-autophosphorylation and leads to the post-transcriptional splicing of X-box binding protein (XBP1) from XBP1s, which then translocate to the nucleus and increase the synthesis of lipids and ER chaperones (Xiao et al., 2017b). The phosphorylation of IRE1α and the expression of XBP1s were significantly increased after deltamethrin treatment compared to the control (38% and 50%, $P = 0.0057$ and 0.0011, respectively, Fig. 4A & DE). CHOP expression is markedly increased in response to ER stress through IRE1-and ATF6-dependent transcription induction (Nishitoh, 2011). Consistently, the expression of CHOP was also markedly increased by deltamethrin treatment (50%, $P = 0.0085$, Fig. 4A & F). These results suggest that deltamethrin induced ER stress in 3T3-L1 adipocytes.

3.4. The chemical chaperone, 4-phenylbutyrate, inhibited adipogenesis induced by deltamethrin in 3T3-L1 adipocytes

4-PBA, a well-established chemical chaperone and inhibitor of ER stress, was reported to inhibit adipogenesis and reduce weight gain in a diet-induced obesity mouse model (Basseri et al., 2009). As shown in Fig. 5A-C, there were significant interactions between deltamethrin and 4-PBA on BiP and CHOP ($P < 0.0001$ for both). As shown in Fig. 5A–D, In the presence or absence of deltamethrin, 4-PBA reduced the expression of pIRE1 (56% and 57%, $P < 0.0001$ and $P = 0.0129$, respectively), BiP (71% and 86%, $P < 0.0001$ and $P = 0.0004$, respectively) and CHOP (70% and 79%, $P < 0.0001$ and $P = 0.0008$, respectively), suggesting the alleviation of ER stress by 4-PBA. Moreover, deltamethrin-induced fat accumulation, C/EBPα, FAS over-expression ($P < 0.0001$ for all three) and AMPK phosphorylation decline ($P = 0.0004$) were abolished by 4-PBA co-treatment as shown in Fig. 5A & E-H. The results indicate that deltamethrin regulates fat accumulation and AMPK phosphorylation via ER stress-mediated pathway.

3.5. Deltamethrin treatment induced ER stress in C. elegans

We further determined the influence of deltamethrin on ER stress in *C. elegans*. *C. elegans* have no mesoderm-derived adipose cells, instead the fat are primarily stored in their intestinal and skin-like epidermal cells (Mullaney and Ashrafi, 2009). In this vein, we investigated the induction of ER stress response with a SJ4005 strain with an *hsp-4p::GFP* reporter. *Hsp-4* is the homolog of mammalian ER chaperone BiP, which is used as a general marker of ER stress response in *C. elegans* (Wang and Kaufman, 2012). During ER stress, *hsp-4* expression is up-regulated and the GFP intensity in SJ4005 worms is higher in the gut and hypodermis than those without ER stress (Hou et al., 2014). The expression of the *hsp-4 GFP* reporter was thus measured to determine ER stress response in *C. elegans*. In this experiment, a 4-h treatment of 3 mM dithiothreitol (DTT), an ER stress inducer, was used as a positive control (Yorimitsu et al., 2006). As shown in Fig. 6A &C, treatment with 25 μM deltamethrin increased the ER stress response significantly by 44% compared to the control ($P = 0.0215$). Since the induction of ER stress in *C. elegans* is usually associated with the accumulation of unfolded and misfolded proteins, the effect of deltamethrin on protein misfolding was also examined using a *C. elegans* polyglutamine model (Angeli et al., 2014). Due to a lack of *C. elegans* polyglutamine aggregates GFP strains in adipose tissue, we studied the influence of deltamethrin on polyglutamine aggregates in *C. elegans* muscle with the *C. elegans* transgenic strain AM141 expressing Q40:YFP in its body wall muscle cells (Angeli et al., 2014) as expression of polyglutamine stretch leads to the formation of aggregation that can be visualized by fluorescent microscopy (Morley et al., 2002). Our results showed that treatment with 25 μM of deltamethrin had no significant effect on the

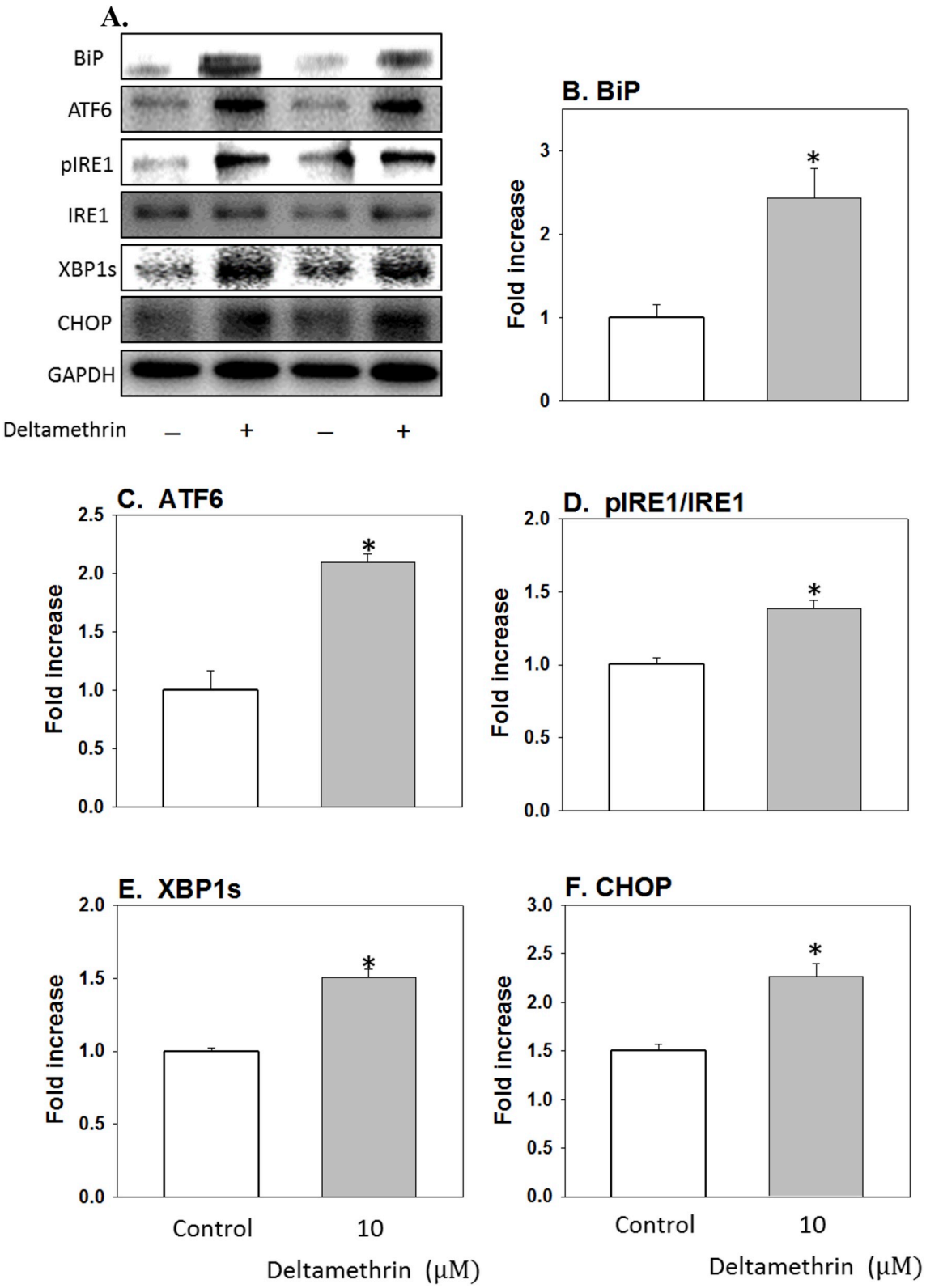

Fig. 4. Effects of deltamethrin on protein levels of ER stress markers. A. representative picture; B. BiP, binding immunoglobulin protein; C. ATF6, activating transcription factor 6; D. pIRE1α/IRE1α, phosphorylated inositol-requiring enzyme 1 α over IRE1α; E. XBP1s, X-box binding protein 1s; and F. CHOP, CCAAT-enhancer-binding protein homologous protein. Cells were treated with deltamethrin (10 μM) for 8 days (from day 0). Numbers represent mean ± S.E. (n = 3–4). * $P < 0.05$, *vs*. control.

average number of polyglutamine aggregates (Fig. 6B & D), but significantly increased the average size of polyglutamine aggregates by 500% ($P < 0.0001$, Fig. 6B & E). These results suggest that deltamethrin induced ER stress in *C. elegans* intestine, hypodermis and muscle.

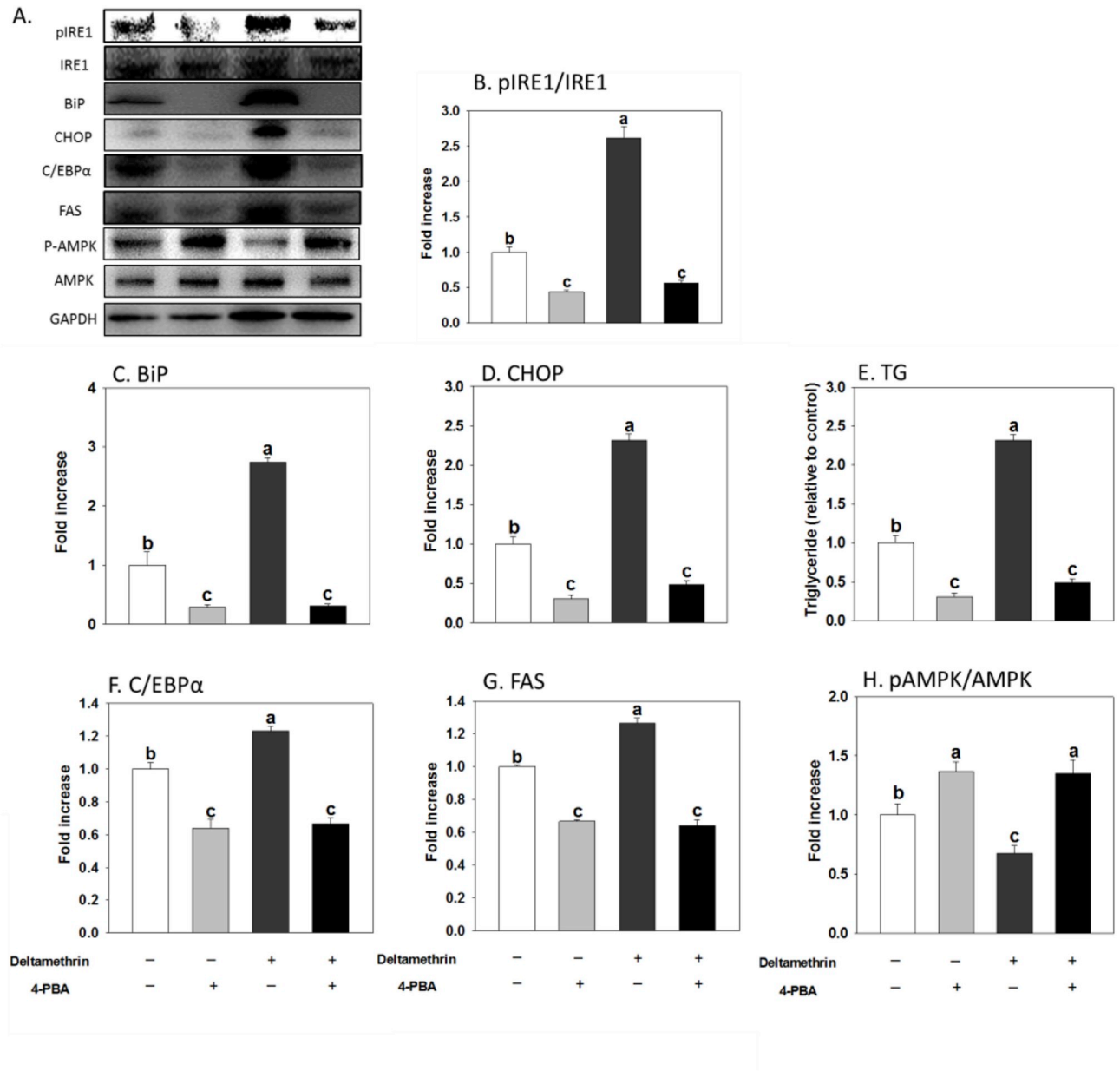

Fig. 5. 4-PBA (4-phenylbutyrate) abolished deltamethrin induced adipogenesis and AMPK phosphorylation in 3T3-L1 adipocytes. A. representative picture; B. pIRE1α/IRE1α, phosphorylated inositol-requiring enzyme 1 α over IRE1α; C. BiP, binding immunoglobulin protein; D. CHOP, CCAAT-enhancer-binding protein homologous protein; E. Triglyceride; F. C/EBPα, CAATT element binding protein-α; G. FAS, Fatty acid synthase; H. pAMPKα/AMPKα, phosphorylated AMP-activated protein kinase-α over AMPKα. Cells were treated with deltamethrin (10 μM) for 8 days (from day 0). Numbers represent mean ± S.E. (n = 3–4). Means with different letters were significantly different at $P < 0.05$.

4. Discussion

The current study suggests that AMPKα and ER stress are involved in increased adipogenesis induced by deltamethrin. This is consistent with the observation that deltamethrin potentiate adipogenesis via an AMPK-dependent mechanism (Shen et al., 2017), and further expands our understanding that ER stress is involved in increased adipogenesis induced by deltamethrin.

AMPK is a master regulator which has a critical role in the regulation of energy balance and lipid metabolism (Bijland et al., 2013). It is known that activation of AMPK inhibits adipogenesis by decreasing the expression of C/EBPα, PPARγ and late adipogenic markers, such as FAS and ACC (Habinowski and Witters, 2001). Our current results indicate that deltamethrin augments fat accumulation through post-translational regulation of AMPK, which is consistent with the previous report that deltamethrin might potentiate adipogenesis in *C. elegans* (Shen et al., 2017).

ER stress has also been linked to obesity and insulin resistance in many previous studies (Basseri et al., 2009; Hotamisligil, 2005; Hummasti and Hotamisligil, 2010; Ozcan et al., 2004). There are three different ER stress pathways with three different ER stress transducers: PERK, IRE1α, and ATF6. These transducers bind to ER chaperones such as BiP under normal conditions. However, under ER stress conditions, BiP dissociates from IRE1, PERK, and ATF6, activating these ER stress transducers (Ron and Walter, 2007). ATF6 is located in the ER membrane and is closely related to lipid biosynthesis (Bommiasamy et al., 2009; Cnop et al., 2012). IRE1α is activated by autophosphorylation (Ron and Walter, 2007), which subsequently results in the translation of XBP1s (Cnop et al., 2012). The IRE1α-XBP1s pathway has also been reported to be indispensable for adipogenesis (Sha et al., 2009).

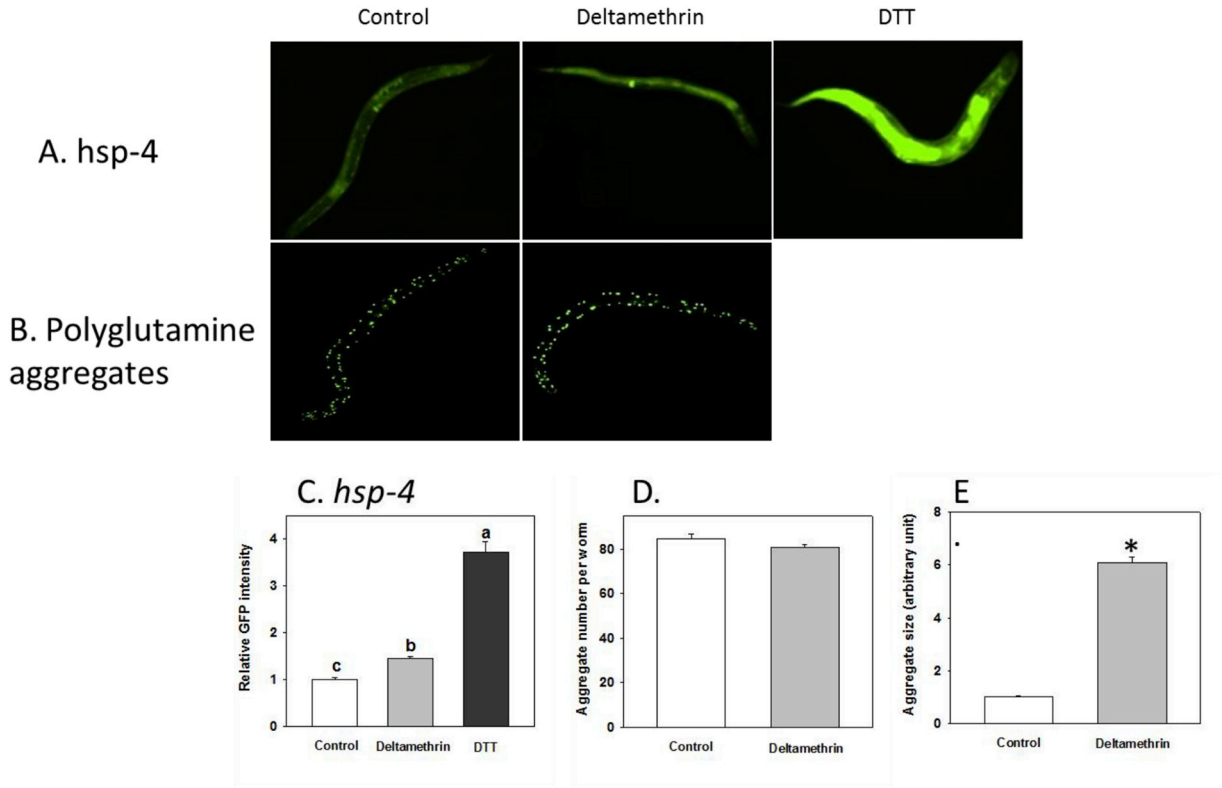

Fig. 6. Effects of deltamethrin on ER stress response. A. Representative images of SJ4005 worms (100 times magnification) on day 3 with control, deltamethrin and dithiothreitol (DTT) treatments; B. Representative images of *AM141* expressing Q40:YFP (100 times magnification); C. The relative GFP intensity of *hsp-4*; D. The number of polyglutamine aggregations counted from YFP images; E. The average size of polyglutamine aggregation counted from YFP images. Treatment of deltamethrin started from L1 stage for three days. The data are described as means ± S.E. (control n = 29, deltamethrin n = 36, DTT n = 69). Means with different letters are significantly different at $P < 0.05$; * $P < 0.05$, *vs.* control.

Previously, it was reported that permethrin (a Type I pyrethroid) induced ER stress, such as the enhanced phosphorylation of IRE1 and the increased expression of BiP, CHOP and XBP1s (Xiao et al., 2017b). Our current results are consistent with these previously reported findings in that deltamethrin treatment likewise increased the expression of BiP, ATF6, XBP1s, CHOP and the phosphorylation of IRE1 in adipocytes. The effect of deltamethrin in causing ER stress was further confirmed in the *C. elegans* model where deltamethrin increased *Hsp-4* expression and the aggregation of polyglutamine. We further observed that 4-PBA inhibited both deltamethrin-induced adipogenesis and AMPK phosphorylation as previously reported in skeletal muscle (Bohnert et al., 2016), suggesting that deltamethrin regulates adipogenesis via an ER stress-AMPK mediated pathway. However, more experiments about 4-PBA, AICAR and their combinational effect in *C. elegans* would be needed further to strengthen the current findings. Given that it is not clear if deltamethrin regulates adipogenesis through ATF6 or the IRE1-XBP1s pathway; this also need to be further explored in the future.

Pyrethroids are known to act on VSSC (voltage-sensitive sodium channels), causing the prolongation of sodium ion influx, and leading to plasma membrane depolarization (Narahashi, 1992). The depolarization of the plasma membrane will open both low- and high-voltage-activated voltage-sensitive calcium channels (VSCC) and allow calcium ion influx (Scamps et al., 2004). Recently, it was also reported that voltage-dependent intracellular calcium transients were caused by the entry of calcium ions through both plasma VSCC and calcium ion release from intracellular stores of the ER via calcium-induced calcium release (CICR) mechanisms (Scamps et al., 2004). ER calcium release has been reported to trigger ER stress and the UPR due to mis-folding of proteins because chaperones require high calcium levels to properly function (Berridge, 1995; Xu et al., 2017). Based on increased ER stress markers and previous reports that pyrethroid insecticides increased intracellular levels, it is possible that deltamethrin induced ER stress via ER calcium release mechanisms; this needs to be further explored in the future.

The toxicity symptom of deltamethrin includes hyperexcitability, paresthesia, tremor, salivation, etc. (Shen et al., 2017). The acceptable daily intake (ADI) of deltamethrin was 0–0.01 mg/kg bw/day in a 1-year study in dogs treated with capsule, a 2-year study in the diet in dogs, and two 2-year studies in the diet in rats (Shen et al., 2017). There is very limited information about the blood concentration of deltamethrin; however, it was reported that deltamethrin residues in human blood, ranging from undetectable to 2–79 μM (Ahmed Azmi and Naqvi, 2011). Thus, the deltamethrin concentration used in the current study might be relevant for human exposure.

In summary, the current study suggests that deltamethrin promoted adipogenesis via an ER stress-AMPK mediated pathway in adipocytes and is significant in providing a potential link between insecticide exposure-deltamethrin in particular-and impaired adipocyte functions. Nonetheless, our current results are limited to cell and *C. elegans* models. Thus, further mice and epidemiological studies are necessary to further elucidate the significance of the current study.

Declaration of interests

The authors declare that they have no known competing financial interests or personal relationships that could have appeared to influence the work reported in this paper.

Acknowledgements

There is no conflict of interest. This project is supported by the National Natural Science Foundation of China (31741104 & 31801641)

and Senior Talent Cultivation Program of Jiangsu University (18JDG023). All the strains were provided by the CGC, which is funded by NIH Office of Research Infrastructure Programs (P40OD010440). We thank Dr. Ying Dong from Jiangsu University for the generosity of giving us full access to their cell culture laboratory. We also want to thank Dr. Hesham EI-Seedi for proofreading the manuscript.

Appendix A. Supplementary data

Supplementary data to this article can be found online at https://doi.org/10.1016/j.fct.2019.110791.

References

Azmi, M.A., Naqvi, S.N.H., 2011. Pesticide pollution, resistance and Health hazards. https://www.intechopen.com/books/pesticides-the-impacts-of-pesticides-exposure/pesticide-pollution-resistance-and-health-hazards.
Anadon, A., Martinez-Larranaga, M.R., Fernandez-Cruz, M.L., Diaz, M.J., Fernandez, M.C., Martinez, M.A., 1996. Toxicokinetics of deltamethrin and its 4'-HO-metabolite in the rat. Toxicol. Appl. Pharmacol. 141, 8–16.
Angeli, S., Barhydt, T., Jacobs, R., Killilea, D.W., Lithgow, G.J., Andersen, J.K., 2014. Manganese disturbs metal and protein homeostasis in Caenorhabditis elegans. Metall 6, 1816–1823.
Armstrong, L.E., Driscoll, M.V., Donepudi, A.C., Xu, J., Baker, A., Aleksunes, L.M., Richardson, J.R., Slitt, A.L., 2013. Effects of developmental deltamethrin exposure on white adipose tissue gene expression. J. Biochem. Mol. Toxicol. 27, 165–171.
Basseri, S., Lhoták, S., Sharma, A.M., Austin, R.C., 2009. The chemical chaperone 4-phenylbutyrate inhibits adipogenesis by modulating the unfolded protein response. J. Lipid Res. 50, 2486–2501.
Berkowitz, G.S., Obel, J., Deych, E., Lapinski, R., Godbold, J., Liu, Z., Landrigan, P.J., Wolff, M.S., 2003. Exposure to indoor pesticides during pregnancy in a multiethnic, urban cohort. Environ. Health Perspect. 111, 79–84.
Berridge, M.J., 1995. Capacitative calcium entry. Biochem. J. 312 (Pt 1), 1–11.
Bijland, S., Mancini, Sarah J., Salt, Ian P., 2013. Role of AMP-activated protein kinase in adipose tissue metabolism and inflammation. Clin. Sci. 124, 491–507.
Bohnert, K.R., Gallot, Y.S., Sato, S., Xiong, G., Hindi, S.M., Kumar, A., 2016. Inhibition of ER stress and unfolding protein response pathways causes skeletal muscle wasting during cancer cachexia. FASEB J. 30, 3053–3068.
Bommiasamy, H., Back, S.H., Fagone, P., Lee, K., Meshinchi, S., Vink, E., Sriburi, R., Frank, M., Jackowski, S., Kaufman, R.J., Brewer, J.W., 2009. ATF6 alpha induces XBP1-independent expansion of the endoplasmic reticulum. J. Cell Sci. 122, 1626–1636.
Choi, J.S., Soderlund, D.M., 2006. Structure-activity relationships for the action of 11 pyrethroid insecticides on rat Na v 1.8 sodium channels expressed in Xenopus oocytes. Toxicol. Appl. Pharmacol. 211, 233–244.
Cnop, M., Foufelle, F., Velloso, L.A., 2012. Endoplasmic reticulum stress, obesity and diabetes. Trends Mol. Med. 18, 59–68.
Gammon, D.W., Brown, M.A., Casida, J.E., 1981. Two classes of pyrethroid action in the cockroach. Pestic. Biochem. Physiol. 15, 181–191.
Habinowski, S.A., Witters, L.A., 2001. The effects of AICAR on adipocyte differentiation of 3T3-L1 cells. Biochem. Biophys. Res. Commun. 286, 852–856.
Ho, N., Xu, C., Thibault, G., 2018. From the unfolded protein response to metabolic diseases - lipids under the spotlight. J. Cell Sci. 131.
Hotamisligil, G.S., 2005. Role of endoplasmic reticulum stress and c-Jun NH2-terminal kinase pathways in inflammation and origin of obesity and diabetes. Diabetes 54 (Suppl. 2), S73–S78.
Hou, N.S., Gutschmidt, A., Choi, D.Y., Pather, K., Shi, X., Watts, J.L., Hoppe, T., Taubert, S., 2014. Activation of the endoplasmic reticulum unfolded protein response by lipid disequilibrium without disturbed proteostasis in vivo. P. Natl. Acad. Sci. USA 111, E2271–E2280.
Hummasti, S., Hotamisligil, G.S., 2010. Endoplasmic reticulum stress and inflammation in obesity and diabetes. Circ. Res. 107, 579–591.
Kim, J., Park, Y., Yoon, K.S., Clark, J.M., Park, Y., 2014. Permethrin alters adipogenesis in 3T3-L1 adipocytes and causes insulin resistance in C2C12 myotubes. J. Biochem. Mol. Toxicol. 28, 418–424.
Kim, J., Sun, Q., Yue, Y., Yoon, K.S., Whang, K.Y., Marshall Clark, J., Park, Y., 2016. 4,4'-Dichlorodiphenyltrichloroethane (DDT) and 4,4'-dichlorodiphenyldichloroethylene (DDE) promote adipogenesis in 3T3-L1 adipocyte cell culture. Pestic. Biochem. Physiol. 131, 40–45.
Kim, K.B., Anand, S.S., Kim, H.J., White, C.A., Bruckner, J.V., 2008. Toxicokinetics and tissue distribution of deltamethrin in adult Sprague-Dawley rats. Toxicol. Sci. 101, 197–205.
Kim, K.B., Anand, S.S., Kim, H.J., White, C.A., Fisher, J.W., Tornero-Velez, R., Bruckner, J.V., 2010. Age, dose, and time-dependency of plasma and tissue distribution of deltamethrin in immature rats. Toxicol. Sci. 115, 354–368.
Lowe, C.E., Dennis, R.J., Obi, U., O'Rahilly, S., Rochford, J.J., 2012. Investigating the involvement of the ATF6α pathway of the unfolded protein response in adipogenesis. Int. J. Obes. 36, 1248–1251.
Mangum, L.H., Howell 3rd, G.E., Chambers, J.E., 2015. Exposure to p,p'-DDE enhances differentiation of 3T3-L1 preadipocytes in a model of sub-optimal differentiation. Toxicol. Lett. 238, 65–71.
Merrill, G.F., Kurth, E.J., Hardie, D.G., Winder, W.W., 1997. AICA riboside increases AMP-activated protein kinase, fatty acid oxidation, and glucose uptake in rat muscle. Am. J. Physiol. 273, E1107–E1112.
Morgan, M.K., Sheldon, L.S., Croghan, C.W., Jones, P.A., Chuang, J.C., Wilson, N.K., 2007. An observational study of 127 preschool children at their homes and daycare centers in Ohio: environmental pathways to cis- and trans-permethrin exposure. Environ. Res. 104, 266–274.
Morley, J.F., Brignull, H.R., Weyers, J.J., Morimoto, R.I., 2002. The threshold for polyglutamine-expansion protein aggregation and cellular toxicity is dynamic and influenced by aging in Caenorhabditis elegans. P. Natl. Acad. Sci. USA 99, 10417–10422.
Mullaney, B.C., Ashrafi, K., 2009. C. elegans fat storage and metabolic regulation. Biochim. Biophys. Acta 1791, 474–478.
Naeher, L.P., Tulve, N.S., Egeghy, P.P., Barr, D.B., Adetona, O., Fortmann, R.C., Needham, L.L., Bozeman, E., Hilliard, A., Sheldon, L.S., 2010. Organophosphorus and pyrethroid insecticide urinary metabolite concentrations in young children living in a southeastern United States city. Sci. Total Environ. 408, 1145–1153.
Narahashi, T., 1992. Nerve membrane Na+ channels as targets of insecticides. Trends Pharmacol. Sci. 13, 236–241.
Nishitoh, H., 2011. CHOP is a multifunctional transcription factor in the ER stress response. J. Biochem. 151, 217–219.
Ozcan, U., Cao, Q., Yilmaz, E., Lee, A.H., Iwakoshi, N.N., Ozdelen, E., Tuncman, G., Gorgun, C., Glimcher, L.H., Hotamisligil, G.S., 2004. Endoplasmic reticulum stress links obesity, insulin action, and type 2 diabetes. Science 306, 457–461.
Park, Y., Kim, Y., Kim, J., Yoon, K.S., Clark, J., Lee, J., Park, Y., 2013. Imidacloprid, a neonicotinoid insecticide, potentiates adipogenesis in 3T3-L1 adipocytes. J. Agric. Food Chem. 61, 255–259.
Peng, Y., Sun, Q., Gao, R., Park, Y., 2019a. AAK-2 and SKN-1 are involved in chicoric-acid-induced lifespan extension in Caenorhabditis elegans. J. Agric. Food Chem.
Peng, Y., Sun, Q., Park, Y., 2019b. Chicoric acid promotes glucose uptake and Akt phosphorylation via AMP-activated protein kinase α-dependent pathway. J. Funct. Foods 59, 8–15.
Peng, Y., Sun, Q., Xu, W., He, Y., Jin, W., Yuan, L., Gao, R., 2019c. Vitexin ameliorates high fat diet-induced obesity in male C57BL/6J mice via the AMPKα-mediated pathway. Food Funct 10, 1940–1947.
Ron, D., Walter, P., 2007. Signal integration in the endoplasmic reticulum unfolded protein response. Nat. Rev. Mol. Cell Biol. 8, 519–529.
Scamps, F., Roig, A., Boukhaddaoui, H., Andre, S., Puech, S., Valmier, J., 2004. Activation of P-type calcium channel regulates a unique thapsigargin-sensitive calcium pool in embryonic motoneurons. Eur. J. Neurosci. 19, 977–982.
Schneider, C.A., Rasband, W.S., Eliceiri, K.W., 2012. NIH Image to ImageJ: 25 years of image analysis. Nat. Methods 9, 671–675.
Sha, H., He, Y., Chen, H., Wang, C., Zenno, A., Shi, H., Yang, X., Zhang, X., Qi, L., 2009. The IRE1alpha-XBP1 pathway of the unfolded protein response is required for adipogenesis. Cell Metabol. 9, 556–564.
Shen, J., Chen, X., Hendershot, L., Prywes, R., 2002. ER stress regulation of ATF6 localization by dissociation of BiP/GRP78 binding and unmasking of Golgi localization signals. Dev. Cell 3, 99–111.
Shen, P., Hsieh, T.H., Yue, Y., Sun, Q., Clark, J.M., Park, Y., 2017. Deltamethrin increases the fat accumulation in 3T3-L1 adipocytes and Caenorhabditis elegans. Food Chem. Toxicol. 101, 149–156.
Sun, Q., Lin, J., Peng, Y., Gao, R., Peng, Y., 2018a. Flubendiamide enhances adipogenesis and inhibits AMPKalpha in 3t3-L1 adipocytes. Molecules 23.
Sun, Q., Qi, W., Xiao, X., Yang, S.H., Kim, D., Yoon, K.S., Clark, J.M., Park, Y., 2017. Imidacloprid promotes high fat diet-induced adiposity in female C57BL/6J mice and enhances adipogenesis in 3t3-L1 adipocytes via the AMPK alpha-mediated pathway. J. Agric. Food Chem. 65, 6572–6581.
Sun, Q., Qi, W., Yang, J.J., Yoon, K.S., Clark, J.M., Park, Y., 2016a. Fipronil promotes adipogenesis via AMPKalpha-mediated pathway in 3T3-L1 adipocytes. Food Chem. Toxicol. 92, 217–223.
Sun, Q., Yue, Y., Shen, P., Yang, J.J., Park, Y., 2016b. Cranberry product decreases fat accumulation in Caenorhabditis elegans. J. Med. Food 19, 427–433.
Sun, Q., Zhang, Z., Zhang, R., Gao, R., McClements, D.J., 2018b. Development of functional or medical foods for oral administration of insulin for diabetes treatment: gastroprotective edible microgels. J. Agric. Food Chem. 66, 4820–4826.
Wang, S.Y., Kaufman, R.J., 2012. The impact of the unfolded protein response on human disease. J. Cell Biol. 197, 857–867.
Xiao, X., Kim, Y., Kim, D., Yoon, K.S., Clark, J.M., Park, Y., 2017a. Permethrin alters glucose metabolism in conjunction with high fat diet by potentiating insulin resistance and decreases voluntary activities in female C57BL/6J mice. Food Chem. Toxicol. 108, 161–170.
Xiao, X., Qi, W., Clark, J.M., Park, Y., 2017b. Permethrin potentiates adipogenesis via intracellular calcium and endoplasmic reticulum stress-mediated mechanisms in 3T3-L1 adipocytes. Food Chem. Toxicol. 109, 123–129.
Xiao, X., Sun, Q., Kim, Y., Yang, S.H., Qi, W., Kim, D., Yoon, K.S., Clark, J.M., Park, Y., 2018. Exposure to permethrin promotes high fat diet-induced weight gain and insulin resistance in male C57BL/6J mice. Food Chem. Toxicol. 111, 405–416.
Xu, S., Xu, Y., Chen, L., Fang, Q., Song, S., Chen, J., Teng, J., 2017. RCN1 suppresses ER stress-induced apoptosis via calcium homeostasis and PERK–CHOP signaling. Oncogenesis 6 e304.
Yoon, K.S., Kwon, D.H., Strycharz, J.P., Hollingsworth, C.S., Lee, S.H., Clark, J.M., 2008. Biochemical and molecular analysis of deltamethrin resistance in the common bed bug (Hemiptera: cimicidae). J. Med. Entomol. 45, 1092–1101.
Yorimitsu, T., Nair, U., Yang, Z., Klionsky, D.J., 2006. Endoplasmic reticulum stress triggers autophagy. J. Biol. Chem. 281, 30299–30304.